International Journal of Control, Automation, and Systems (2011) 9(5):913-923 http://www.springer.com/12555
DOI 10.1007/s12555-011-0512-9

A Computational Neuromusculoskeletal Model of Human Arm Movements

Sungho Jo

Abstract: This work proposes a computational neuromusculoskeletal model of human arm movements. The model consists of three components: the supraspinal neural control system, the spinal motor system, and the muscle-tendon actuation system. In the supraspinal neural system model, the cerebellum is regarded as having feedforward control and the cerebrum as feedback control principally based on the feedback-error learning scheme. This computational model proposes that the feedforward control of the cerebellum may not need to be an explicit locus of an inverse dynamic model. This model also includes the modularly organized spinal motor system such that it simplifies controlling redundant muscular actuators. Cerebellar feedforward control and the spinal motor system are assumed to be adaptive. The two motor adaptations seem to synergistically promote motion flexibility and simplify the neural system structure. The neural control system is combined with the Hill-type muscle-tendon model to generate arm movement. The overall model proposes that an approximate inverse dynamic model may implicitly be constructed over the integrated neuromusculoskeletal system, and it is not necessary to be explicitly computed in a specific motor system. To cope with the human neural system, neuromuscular activation dynamics and neural transmission delays are included in the model. A computational simulation study using the model was implemented to verify the feasibility of the model. Center out reaching movements and learning of those movements as well s generations of figure eight-like movements were computationally tested. A plausible motor control scheme of movement is discussed using the model.

Keywords: Feedback error learning, Hill-type muscle-tendon model, human arm movements, spinal synergy.

1. INTRODUCTION

How the human nervous system generates movements is a challenging question. The role of the cerebellum in the control of arm reaching movements especially requires more scientific scrutiny because the cerebellum is known to coordinate and control posture and movement and to implement motor learning. Cerebellar neuronal processing has been intensively investigated in the neuroscience society. From the perspective of engineering control theory, the cerebellar neural mechanism of controlling movements can be regarded as feedback or feedforward control [1]. It has been argued that neural feedback control of human movement is limited by the long delays and dynamic properties of muscle proprioceptors. Instead, feedforward control can avoid the effect of the delays and can produce fast movements that are not dependent on afferent information from muscles. However, feedforward control may require the inverse dynamics information of the skeletal system over a relevant frequency range, which leads to the necessity of a complicated neural computation. Computational studies have demonstrated that precise inverse dynamics are not necessary, that an approximate inverse model may be sufficient [2-5], and that a combination feedback and feedforward control scheme may be essential [6]. The existence of neural implementation of feedback and feedforward controllers has been difficult to show at a cellular level, but Gomi and Kawato have investigated it and proposed a model called feedback error learning (FEL) [4,5]. The FEL model is one of the most popular schemes to explain the function of the cerebellum in motor control and learning.

The spinal motor system has been reinterpreted to be an active participant in adaptive motor learning [7-9]. Because most descending neural signals should pass through the spinal motor system to activate the muscles, the organization of the spinal motor system is critical in the control of movements. Studies by the Bizzi group at MIT have observed that the spinal motor system is organized into a number of distinct 'modular units' of motor outputs, and a combination of the modules produces a range of movements [10-13]. These modular units are termed *Synergies*, which are the basis of functions constructing motor output. Experimentally, decomposition of the muscular activities of frog limb movements resulted in a set of principal waveforms; these activities could be reconstructed from the combination of the principal waveforms. It was also demonstrated that rhythmic motor behaviors such as human walking could be con-

Manuscript received March 3, 2010; revised May 15, 2011; accepted June 17, 2011. Recommended by Editor Young-Hoon Joo. This work was supported by MKE under the Human Resources Development Program for Convergence Robot Specialists and by MEST under KRF grant No. 2010-0015226.

Sungho Jo is with the Department of Computer Science, Korea Advanced Institute of Science and Technology, 291 Daehak-ro, Yuseong-gu, Daejeon 305-701, Korea (e-mail: shjo@kaist.ac.kr).

structed by a small number of principal patterns of synergies in the spinal cord [8,14], and the concept was computationally tested with a human biped walking model [15-17]. The modular organization of the spinal motor system can be regarded as a compact way to summarize motor control space. The reduction to a lower dimensional space helps simplify the control problem with redundant muscular actuators. Interesting questions are whether such a modular neuronal organization really exists in the spinal motor system and, if so, how to adapt the modular sets that represent network connectivity in the spinal motor or the corticospinal network system to implement a specific movement task. At present, psychophysical or physiological experiments have supported the existence of modular organization or motor adaptation in spinal neuronal networks. Experiments on vertebrates such as the turtle, mudpuppy, frog, rat, and cat proposed the existence of neurophysiological modular organization in vertebrate spinal motor systems [10,18-20]. Identification of adaptive spinal motor systems is achieved by experiments on spinalized animal locomotion [7]. Spinalized cats demonstrate a clear adaptation of locomotor patterns in the spinal cord isolated from other nervous systems after specific muscle nerve cuts [21,22]. Human patients with spinal cord injury demonstrate the recovery of locomotor ability; the adaptation process in the spinal motor system has been observed with different patterns of muscular activity before and after training [23].

A typical muscle consists of many thousands of muscle fibers working in parallel. Motor neurons convey descending commands to the muscle fibers. The bundle of muscle fibers innervated by only one motor neuron is called a muscle unit. A single action potential in a motor neuron activates the muscle unit in synchrony. Accumulation of overlapping action potentials results in a complex pattern of electrical potentials, which can be recorded by electromyogram (EMG). A single muscle fiber microscopically contains many myofibrils. The myofibrils in all muscle fibers tend to change length in concert as a result of the various noncontractile components that link them mechanically. This results in a passive spring-like restoring force. It does not require energy consumption but is induced by the mechanical properties of the muscle fibers. The contractile machinery of the filaments also produces contraction by the mechanism of the so-called "sliding filament hypothesis". This is an active energy-consuming process. The contraction of the contractile component can stretch inactive muscle components, which produce the spring-like restoring force. Therefore, the total force produced by a muscle fiber consists of active and passive forces. Contractile force depends on the level of activation of each muscle fiber and its length and velocity. A mathematical model that captures the interrelations between length-to-force, velocity-to-force, and activation level-to-force in the muscle tendon is called the Hill-type model [24,25].

In this paper, a computational neuromusculoskeletal model to learn and control human arm movement is proposed based on the statements above. Through computational tests with the model, a possible mechanism for the motor control and learning process is proposed. In the following section, each component in the overall model is explained individually and integrated. Section three presents computational simulation studies, and the last section discusses a plausible motor control scheme of human movements.

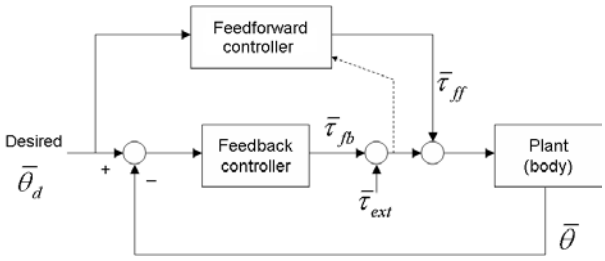

Fig. 1. Diagram of the feedback error learning model.

2. COMPUTATIONAL MODEL

2.1. Supraspinal neural control model

The FEL model is the adaptive control scheme proposed as a computational model of the functional role of the cerebellum [4,5]. To support the algorithm neurophysiologically, theoretical or experimental studies have been conducted [2-5,26-28]. The cerebellum is regarded as a locus of the approximation of plant inverse dynamics. Initially, a crude feedback controller exerts more influence on the operation. However, as the cerebellar system learns the estimation of the plant inverse, the command from the feedforward dominates.

The feedback controller is typically set, for example, as in [2,3,5,29],

$$\bar{\tau}_{fb} = K_1(\ddot{\bar{\theta}}_d - \ddot{\bar{\theta}}) + K_2(\dot{\bar{\theta}}_d - \dot{\bar{\theta}}) + K_3(\bar{\theta}_d - \bar{\theta}). \quad (1)$$

In general, a learning scheme can be expressed by

$$\bar{\tau}_{ff} = \varphi(\bar{\theta}_d, \bar{\theta}, \dot{\bar{\theta}}_d, \dot{\bar{\theta}}, \ddot{\bar{\theta}}_d, \ddot{\bar{\theta}}, W), \quad (2)$$

where W represents the adaptive parameter vector, $\bar{\theta}_d$ the desired position vector, and $\bar{\theta}$ the actual position vector. The adaptive update rule for FEL is

$$\frac{dW}{dt} = \eta\left(\frac{\partial\varphi}{\partial W}\right)^T\left(\bar{\tau}_{fb} + \bar{\tau}_{ext}\right), \quad (3)$$

where $\bar{\tau}_{ext}$ is the external torque and η the learning ratio, which is small. The convergence property of the FEL scheme is shown in [27-29].

In this paper, a modified FEL model is proposed to simulate movements with the Hill-type muscle-tendon model, which is more neurophysiological than general viscoelastic models. The feedforward and feedback commands are described with respect to neural descending signals toward the alpha motorneurons and not joint toques as in the original FEL model.

In the proposed model, each component of the

feedforward and feedback signals is respectively modeled as:

$$\bar{u}_{ff} = W_{C1}\ddot{\bar{\theta}}_d + W_{C2}\dot{\bar{\theta}}_d + W_{C3}\bar{\theta}_d + W_{C4}\dot{\bar{\theta}}_{d\_H}, \quad (4)$$

$$\bar{u}_{fb} = K_{C1}(\ddot{\bar{\theta}} - \ddot{\bar{\theta}}_d) + K_{C2}(\dot{\bar{\theta}} - \dot{\bar{\theta}}_d) + K_{C3}(\bar{\theta} - \bar{\theta}_d). \quad (5)$$

$\bar{u}_{ff}$ is interpreted to be the output from the cerebellar microcomplexes [30]. The desired trajectories $\ddot{\bar{\theta}}_d$, $\dot{\bar{\theta}}_d$, $\bar{\theta}_d$, or second-order terms are inputs through the parallel fibers to the Purkinje cells in the cerebellar cortex [6]. The last term in (5) especially embodies nonlinear components. The 2x2 weight matrices $W_{Ci}(i=1, 2, 3)$ and the 2x3 matrix W_{C4} can be thought of as relative intensities of the Purkinje cells and deep cerebellar nuclei. $\bar{u}_{fb}$ describes the efferent signals generated by the motor cortex. The motor cortical control is designed to be a feedback control representing a crude corrective performance as in [2-5]. This work aims to implement planar arm movements in the horizontal plane. Therefore, the desired shoulder angle (θ_{d1}) and elbow angle (θ_{d2}) trajectories are considered: $\bar{\theta}_d = [\theta_{d1} \quad \theta_{d2}]^T$. Let $\dot{\bar{\theta}}_{d\_H} = [\dot{\theta}_{d1} \quad \dot{\theta}_{d2} \quad \dot{\theta}_{d1}^2 \quad \dot{\theta}_{d2}^2]^T$ describe nonlinear components.

$K_{C1} = 0.002$, $K_{C2} = 0.06$, and K_{C3}=0.2 were chosen empirically for simulations.

The weight matrices $W_{Ci}(i=1, 2, 3)$ were adapted by learning laws as follows

$$\begin{aligned}
&\frac{dW_{C1}}{dt} = -\eta\bar{\theta}_d\bar{u}_{IO}^T, && \frac{dW_{C2}}{dt} = -\eta\dot{\bar{\theta}}_d\bar{u}_{IO}^T,\\
&\frac{dW_{C3}}{dt} = -\eta\ddot{\bar{\theta}}_d\bar{u}_{IO}^T, && \frac{dw_1}{dt} = -\eta\dot{\theta}_{d1}\dot{\theta}_{d2}u_{IO1},\\
&\frac{dw_2}{dt} = -\eta\dot{\theta}_{d1}^2u_{IO1}, && \frac{dw_3}{dt} = -\eta\dot{\theta}_{d2}^2u_{IO1},\\
&\frac{dw_4}{dt} = -\eta\dot{\theta}_{d1}\dot{\theta}_{d2}u_{IO2}, && \frac{dw_5}{dt} = -\eta\dot{\theta}_{d1}^2u_{IO2},\\
&\frac{dw_6}{dt} = -\eta\dot{\theta}_{d2}^2u_{IO2},
\end{aligned} \quad (6)$$

where $W_{C4} = \begin{bmatrix} w_1 & w_2 & w_3 \\ w_4 & w_5 & w_6 \end{bmatrix}$ and $\bar{u}_{IO} = \begin{bmatrix} u_{IO1} \\ u_{IO2} \end{bmatrix}$.

η is a learning coefficient ($\eta = 0.5$), and $\bar{u}_{IO}$ may be comparable with the input signals to Purkinje cells in the cerebellar cortex through the climbing fibers from the inferior olivary (IO) cells [6].

The climbing fiber input $\bar{u}_{IO}$ plays a role in the training error signal modeled as in [2,3,31]

$$\bar{u}_{IO} = K_{E1}(\ddot{\bar{\theta}} - \ddot{\bar{\theta}}_d) + K_{E2}(\dot{\bar{\theta}} - \dot{\bar{\theta}}_d) + K_{E3}(\bar{\theta} - \bar{\theta}_d). \quad (7)$$

Gains $K_{E1} = 0.0002$, $K_{E2} = 0.006$, and $K_{E3} = 0.02$ were chosen for the simulation.

Sensed information, such as $\ddot{\bar{\theta}}$, $\dot{\bar{\theta}}$, and $\bar{\theta}$, can be thought of as afferents from the muscle spindles or the Golgi tendon receptors [3]. The desired state, such as $\ddot{\bar{\theta}}_d$, $\dot{\bar{\theta}}_d$, $\bar{\theta}_d$ probably comes from the cerebral cortex. Then neural delay between the afferent and the desired exists. The phasic mismatch would cause an incorrect estimation of the inverse model. The incorrect estimation may not be a large problem to generate slow movements, but it seriously leads to bad performance in the case of fast movements. A possible resolution [31,32] is that the desired state is established in muscle spindles through direct gamma motorneuron signaling to the spinal segments. The error is then detected at the low latency reflex feedback circuit and sent to the IO cells; therefore, a functionally significant delay is present. Another possibility is that the transmission of the desired state from the cortical cortex to the IO cells experiences neural processing with approximately the same delay as the sensed afferent transmission [2,3]; therefore, the time difference is practically negligible between the two signals.

2.2. Spinal motor system

The descending signal from the supraspinal system is distributed to alpha motorneurons via the spinal motor system. A simple network model is:

$$\bar{u} = W_S\bar{u}_s, \quad (8)$$

where W_S is a weight matrix representing either the spinal neuronal or cerebral cortical area 4 (MI) network as argued in [33] or an overall distribution network through the corticospinal pathway. Each element in the matrix can be negative, positive or zero, where the sign represents an inhibitory or excitatory connection and zero represents no connection.

The role of distributive network W_S allows a fewer number of descending neural commands to actuate a higher number of muscles. To emphasize the spinal synergy mentioned in the introduction section, this study assumes that W_S represents the spinal synergy distributive network. Computational studies have demonstrated its effectiveness in control of redundant actuators [15-17]. In the proposed model, the spinal neuronal network is considered to be an active adaptive motor system [7]. Therefore, W_s can be adapted.

In this model, the Oja's update rule describes the spinal motor adaptation:

$$\frac{dW_S}{dt} = \eta_s(W_S\bar{u}_s\bar{u}_s^T - \overline{uu}^TW_S) = \eta_s(\overline{uu}_s^T - \overline{uu}^TW_S), \quad (9)$$

where η is a learning coefficient ($\eta_S = 0.02$ for simulation).

The first term in the parenthesis on the right hand is the Hebbian rule. Hebbian learning has been interpreted as synaptic plasticity in the form of both long-term potentiation and depression [34]. The second term is the normalization effect to avoid a diverging weight. Oja's rule is, from a different perspective, finding principal components of the covariance matrix of the input. In this way, information is summarized into directions of the few largest eigenvectors. Thus, a few principal vectors

can effectively span the input space. Hebbian learning is a well-known rule that represents the firing learning mechanism of the presynaptic and postsynaptic neurons.

In the present study, the rule seems the most biologically plausible to describe the spinal motor adaptation [34] because, at least at present, neither the specific error-driven learning scheme nor the neuronal network is neuroanatomically shown in the spinal system. The rule is presented in a simple form to represent neuronal computation, and evidence of such mechanisms for neuronal adaptation has been suggested [34-37]. It has been experimentally observed that the regulation of synaptic activity in spinal cord neurons results in a long-term modulation of excitatory synaptic transmission [37].

2.3. Skeletal arm and muscle-tendon actuator model

Human arm dynamics of planar motions in a horizontal plane are represented by a two-segment, 2 degree-of-freedom linkage as in Fig. 2. Positive angular motion is consistent with anatomical flexion at both shoulder and elbow joints. The arm is actuated by six muscle-tendon actuators (discussed below).

The arm consists of the upper arm and the forearm segments. The skeletal dynamics are described as:

$$\bar{T} = M(\bar{\theta})\ddot{\bar{\theta}} + N(\bar{\theta},\dot{\bar{\theta}}) + R(\bar{\theta}) + V(\dot{\bar{\theta}}), \tag{10}$$

where $M(\bar{\theta})$ is the 2x2 inertia matrix and $N(\bar{\theta},\dot{\bar{\theta}})$ is the 2x1 Coriolis and centrifugal vector.

$$M(\bar{\theta}) = \begin{bmatrix} m_1 r_1^2 + m_2(l_1^2 + r_2^2 + 2l_1 r_2 \cos\theta_2) + I_1 + I_2 & m_2(r_2^2 + l_1 r_2 \cos\theta_2) + I_2 \\ m_2(r_2^2 + l_1 r_2 \cos\theta_2) + I_2 & m_2 r_2^2 + I_2 \end{bmatrix} \tag{11}$$

and

$$N(\bar{\theta},\dot{\bar{\theta}}) = -m_2 l_1 r_2 \sin\theta_2 \begin{bmatrix} \dot{\theta}_2(2\dot{\theta}_1 + \dot{\theta}_2) \\ -\dot{\theta}_1^2 \end{bmatrix}, \tag{12}$$

where m_i, I_i, l_i, and r_i arethe mass, the moment of inertia, the length, and the distance to the center of mass from the adjacent joint of each segment (i=1: upper arm, i=2: forearm+hand),respectively, θ_1 is the shoulder angle and θ is the elbow angle as in Fig. 2. Table 1 summarizes the physical parameters used to describe the human arm.

$R(\bar{\theta})$ and $V(\dot{\bar{\theta}})$ are the 2x1 vectors representing the torques exerted by the passive elastic and viscous properties of joint capsules and ligaments, respectively, which restrict the ranges of joint motions [38,39].

$$R(\bar{\theta}) = \begin{bmatrix} -\alpha_{11}\exp(-\beta_{11}(\theta_1 - \phi_{11})) + \alpha_{12}\exp(\beta_{12}(\theta_1 - \phi_{12})) \\ -\alpha_{21}\exp(-\beta_{21}(\theta_2 - \phi_{21})) + \alpha_{22}\exp(\beta_{22}(\theta_2 - \phi_{22})) \end{bmatrix}, \tag{13}$$

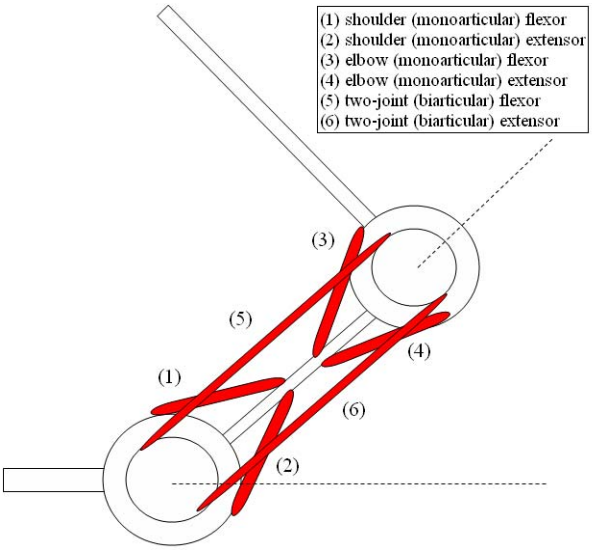

(a) Schematic representation of the muscle attachments; the numbersare consistent with the muscle list in Table 1.

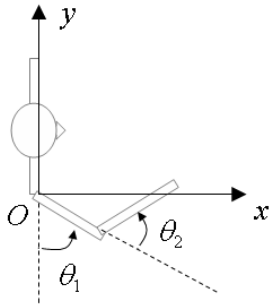

(b) Joint convention of the arm model (θ_1: shoulder angle, θ_2: elbow angle).

Fig. 2. Joint and muscle configuration used for the estimation study.

Table 1. Physical parameters of the skeletal arm model. The values are adapted from [39,40].

	m_i (kg)	I_i (kgm^2)	l_i (m)	r_i (m)
i=1: upper arm	1.93	0.0477	0.33	0.18
i=2: forearm	1.52	0.0588	0.35	0.20

Table 2. Physical parameters of the passive joint properties. The values were adapted from [38, 40].

	α_{i1}	α_{i2}	β_{i1}	β_{i2}	ϕ_{i1}	ϕ_{i2}	γ_i
i=1	0.0008	2.79	1.75	1.96	3.67	1.05	1.6
i=2	1.41	1.41	7.29	7.29	-0.046	2.3	0.8

$$V(\dot{\bar{\theta}}) = \begin{bmatrix} \gamma_1\dot{\theta}_1 \\ \gamma_2\dot{\theta}_2 \end{bmatrix}. \tag{14}$$

Relevant parameters are summarized in Table 2.

To move the planar skeletal arm, four mono-articular and two bi-articular muscles were attached around the joints as in Fig. 2. The contractile element (CE) of each muscle generates force depending on the maximum isometric force ($F_{\max,i}$), force-velocity property, force-length property, and muscular activation (*act*) [25,41].

$$F_{CE,i}(act_i, \dot{l}_{CE,i}, l_{CE,i}) = act_i F_{\max,i} f_{v,i}(\dot{l}_{CE,i}) f_{l,i}(l_{CE,i}) \quad \text{for} \quad i = 1,...,6, \quad (15)$$

where $0 \le act_i \le 1$ and i indicates the corresponding muscle in Fig. 2.

The force-length property was expressed as in [42-44]:

$$f_{l,i}(l_{CE,i}) = \exp\left(c \left| \frac{l_{CE,i} - l_{opt,i}}{l_{opt,i} w} \right|^3 \right), \quad (16)$$

where l_{opt} is the optimum contractile element length for maximum force production, w determines the width of $f_l(l_{CE})$ ($w = 0.4$), and c is a coefficient ($c = \ln(0.05)$).

The force-velocity property is characterized depending on whether the muscle shortens or lengthens [42-44].

$$f_{v,i}(\dot{l}_{CE,i}) = \begin{cases} \dfrac{v_{\max,i} - \dot{l}_{CE,i}}{v_{\max,i} + K\dot{l}_{CE,i}}, & \text{if } \dot{l}_{CE,i} < 0 \\ N + (N-1)\dfrac{v_{\max,i} + \dot{l}_{CE,i}}{7.56K\dot{l}_{CE,i} - v_{\max,i}}, & \text{if } \dot{l}_{CE,i} \ge 0, \end{cases} \quad (17)$$

where $v_{\max,i}$ is a maximum shortening velocity and isset to $-12 l_{opt,i}$, N is the dimensionless value of $F_{CE,i} / F_{\max,i}$ with a lengthening velocity of $\dot{l}_{CE,i} = -v_{\max,i}$ (N=1.5 for computation), and K is a curvature constant and is set to 5.

The serial elastic element (SE) is usually characterized by a nonlinear elastic force-length property [42-44]:

$$f_{SE,i}(l_{SE,i}) = \begin{cases} \left(\dfrac{l_{SE,i} - l_{slack,i}}{\varepsilon l_{slack,i}} \right)^2, & \text{if } l_{SE,i} > l_{slack,i} \\ 0, & \text{if } l_{SE,i} \le l_{slack,i}, \end{cases} \quad (18)$$

where $l_{slack,i}$ is the tendon slack length and ε represents the relative strain of the SE at maximal isometric force (set to 0.04 for all muscles).

In this computational model, the CE and SE were serially connected. Therefore, the force was balanced as followed under the assumption that muscles remain activated during motions, and the effect of passive elements is negligible [45].

$$F_{M,i} = F_{SE,i} = F_{CE,i}, \quad (19)$$

where $F_{M,i}$ represents the muscle force.

At the same time, the muscle-tendon length ($\bar{l}_{MTC}$) and joint angle ($\bar{\theta}$) hold the following condition geometrically.

The CE length can be calculated using geometric relation,

$$\begin{aligned} &\bar{l}_{MTC} = \bar{l}_{SE} + \bar{l}_{CE} = \bar{l}_o + A^T \bar{\theta} \quad \text{and} \\ &\dot{\bar{l}}_{MTC} = \dot{\bar{l}}_{SE} + \dot{\bar{l}}_{CE} = A^T \dot{\bar{\theta}}, \end{aligned} \quad (20)$$

where $\bar{l}_o$ is the reference length when all joint angles are zero, $\bar{l}_{SE}$ the SE length, $\bar{l}_{CE}$ the CE length, and A the moment arm matrix. It was assumed for simplicity that each muscle is attached with a constant moment arm around a joint.

The values of the model parameters are in Table 3.

Table 3. Parameters for the muscle-tendon model. Each maximal isometric force value was determined considering the pennation angle [40]. The parameter values were adapted from [39,40].

i	(1)	(2)	(3)	(4)	(5)	(6)
$F_{\max,i}$ (N)	1151	990	983	616	625	783
$l_{opt,i}$ (m)	0.14	0.09	0.25	0.11	0.12	0.13
$l_{slack,i}$ (m)	0.1	0.05	0.15	0.09	0.27	0.14
$l_{o,i}$ (m)	0.228	0.19	0.207	0.281	0.331	0.301

The SE length could be described by the CE length and joint angles.

$$\bar{l}_{SE} = \bar{l}_o + A^T \bar{\theta} - \bar{l}_{CE}. \quad (21)$$

Moment arm matrix was set to be:

$$A = \begin{bmatrix} a_1 & -a_2 & 0 & 0 & a_5 & -a_7 \\ 0 & 0 & a_3 & -a_4 & a_6 & -a_8 \end{bmatrix}, \quad (22)$$

where a_1 is the moment arm of the shoulder flexor, a_2 is the shoulder extensor, a_3 is the elbow flexor, a_4 is the elbow extensor, a_5 is the biarticular flexor at the shoulder, a_6 is the biarticular flexor at the elbow, a_7 is the biarticular extensor at the shoulder, and a_8 is the biarticular extensor at the elbow.

From the above relation, when the activation signal a_i activates the muscle,

$$\begin{aligned} \dot{l}_{CE,i} &= f_{v,i}^{-1}\left(\frac{F_{CE,i}(act_i, \dot{l}_{CE,i}, l_{CE,i})}{act_i F_{\max,i} f_{l,i}(l_{CE,i})} \right) \\ &= f_{v,i}^{-1}\left(\frac{F_{SE,i}(l_{SE,i})}{act_i F_{\max,i} f_{l,i}(l_{CE,i})} \right) \\ &= f_{v,i}^{-1}\left(\frac{F_{SE,i}(l_{CE,i})}{act_i F_{\max,i} f_{l,i}(l_{CE,i})} \right), \end{aligned} \quad (23)$$

$$l_{CE,i} = \int_{t_o}^{t} f_{v,i}^{-1}\left(\frac{F_{SE,i}(l_{CE,i})}{act_i F_{\max,i} f_{l,i}(l_{CE,i})} \right) dt. \quad (24)$$

Equations (23) and (24) calculate the CE velocity and length, respectively, recursively in real time. Then (15) represents the generation of muscular force.

The neuromuscular activation (excitation and contraction coupling) dynamics were simply described according to [25].

$$\dot{act}_i + \frac{1}{\tau_{act}}\left(\beta + (1-\beta)u_i\right) act_i = \frac{1}{\tau_{act}} u_i, \quad (25)$$

where $\delta \le act_i \le 1$, τ_{act} is the activation time constant, and τ_{act} / β is the deactivation time constant. The

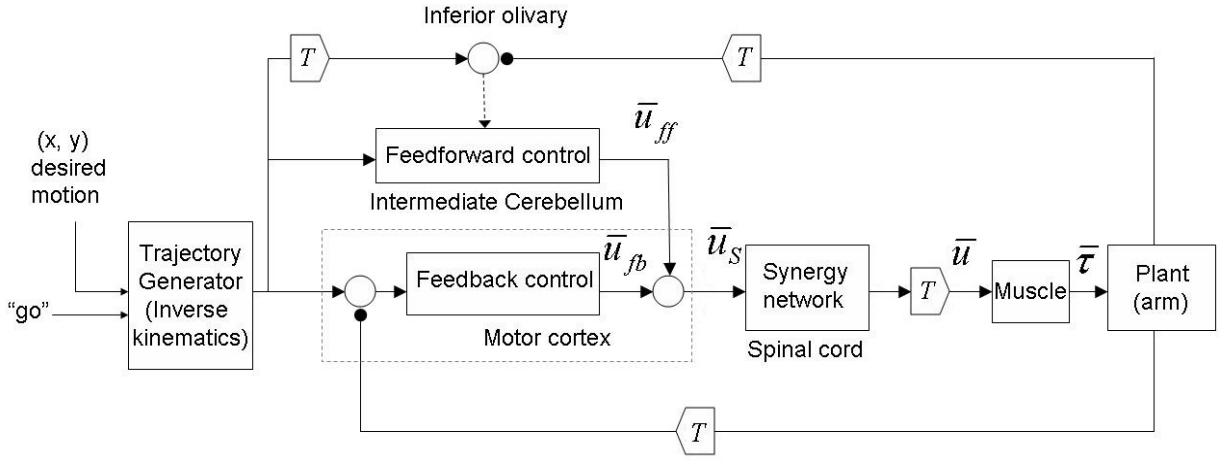

Fig. 3. An adaptive neuromusculoskeletal model of human arm movement.

activation dynamics provide the muscular activation act_i from the descending neural signal u_i. δ is a small value representing baseline activation (δ=0.01 for simulation). The baseline activation prevented the value inside $f_{v,i}^{-1}$ in (24) from being infinity.

Joint torques are then computed as follows:

$$\begin{aligned}\bar{T} &= A^T \bar{F}_{CE}(\overline{act}, \dot{\bar{l}}_{CE}, \bar{l}_{CE}) \\ &= A^T \bar{f}(\bar{F}_{CE,\max}, \dot{\bar{l}}_{CE}, \bar{l}_{CE}) \otimes \overline{act} \\ &= F(\bar{\theta}, \dot{\bar{\theta}})\overline{act}.\end{aligned} \tag{26}$$

From (10) and (26), the musculoskeletal model of the human arm is:

$$M(\bar{\theta})\ddot{\bar{\theta}} + N(\bar{\theta}, \dot{\bar{\theta}}) + R(\bar{\theta}) + V(\dot{\bar{\theta}}) = F(\bar{\theta}, \dot{\bar{\theta}})\overline{act}. \tag{27}$$

The effect of the muscle-tendon system on arm dynamics is proportional to activation $\bar{a}$ under the assumption that the muscles fully activate over a motion [45]. $F(\bar{\theta}, \dot{\bar{\theta}})$ expresses the general force-length-velocity relation.

2.4. Model summary

Fig. 3 illustrates the overall neuromusculoskeletal system. Each *T* indicates a neural transmission delay.

The sum of the two signals from cerebellum and cerebrum descends to the spinal cord network.

$$\bar{u}_s = \bar{u}_{ff} + \bar{u}_{fb}. \tag{28}$$

Therefore, it can be regarded that the neural signals are transformed to a muscular activation signal almost in the form of $\bar{a} \approx W_S(\bar{u}_{ff} + \bar{u}_{fb})$ by neglecting the effect of neuromuscular activation dynamics and neural transmission delays for simplicity. The neuromuscular activation dynamics in (25) lag the descending signals in the manner of a low-pass filter.

By connecting the modified FEL control with the musculoskeletal dynamics from (4), (5), (8), (27), and (28):

$$\begin{aligned}&M(\bar{\theta})\ddot{\bar{\theta}} + N(\bar{\theta}, \dot{\bar{\theta}}) + R(\bar{\theta}) + V(\dot{\bar{\theta}}) \\ &= F(\bar{\theta}, \dot{\bar{\theta}})W_S(\bar{u}_{ff} + \bar{u}_{fb}) \\ &= F(\bar{\theta}, \dot{\bar{\theta}})W_S \\ &\quad \begin{pmatrix} W_{C1}\ddot{\bar{\theta}}_d + W_{C2}\dot{\bar{\theta}}_d + W_{C3}\bar{\theta}_d + \dot{\bar{\theta}}_d^T W_{C4}\dot{\bar{\theta}}_d \\ + K_{C1}(\ddot{\bar{\theta}}_d - \ddot{\bar{\theta}}) + K_{C2}(\dot{\bar{\theta}}_d - \dot{\bar{\theta}}) + K_{C3}(\bar{\theta}_d - \bar{\theta}) \end{pmatrix} \\ &= \underbrace{F(\bar{\theta}, \dot{\bar{\theta}})W_S(W_{C1}\ddot{\bar{\theta}}_d + W_{C2}\dot{\bar{\theta}}_d + W_{C3}\bar{\theta}_d + \dot{\bar{\theta}}_d^T W_{C4}\dot{\bar{\theta}}_d)}_{\bar{\tau}_{ff}} \\ &\quad + \underbrace{F(\bar{\theta}, \dot{\bar{\theta}})W_S(K_{C1}(\ddot{\bar{\theta}}_d - \ddot{\bar{\theta}}) + K_{C2}(\dot{\bar{\theta}}_d - \dot{\bar{\theta}}) + K_{C3}(\bar{\theta}_d - \bar{\theta}))}_{\bar{\tau}_{fb}}.\end{aligned} \tag{29}$$

The formulation above clarifies the feedforward and feedback components from the viewpoint of joint toque.

As long as adaptation schemes successfully converge, i.e., $\bar{\theta} \to \bar{\theta}_d$, then,

$$\begin{aligned}&K_{C1}(\ddot{\bar{\theta}}_d - \ddot{\bar{\theta}}) + K_{C2}(\dot{\bar{\theta}}_d - \dot{\bar{\theta}}) + K_{C3}(\bar{\theta}_d - \bar{\theta}) \to \bar{0}, \\ &F(\bar{\theta}, \dot{\bar{\theta}})W_S W_{C1} \to M(\bar{\theta}_d), \\ &F(\bar{\theta}, \dot{\bar{\theta}})W_S(W_{C2}\dot{\bar{\theta}}_d + W_{C3}\bar{\theta}_d + \dot{\bar{\theta}}_d^T W_{C4}\dot{\bar{\theta}}_d) \\ &\to N(\bar{\theta}_d, \dot{\bar{\theta}}_d) + R(\bar{\theta}) + V(\dot{\bar{\theta}}).\end{aligned}$$

Here, the formulations derived above indicate that the integrated neuronal organizations of the supraspinal, spinal, and muscular systems are identified with nonlinear skeletal dynamics.

3. RESULTS

Some tests of planar arm movements were computationally implemented with the proposed neuromusculoskeletal model. The tests consisted of point-to-point straight reaching movements and curved movements. Model parameters other than adapted ones (W_{Ci} : i =1, 2, 3, 4, and W_S) remained unchanged over the whole tests. For simulations, transmission delays were assigned to be 15 ms and 20 ms for the shoulder and elbow, respectively, at location *T* in Fig. 3.

3.1. Point-to-point reaching movements

A computational study described arm movements to eight radial directions from a central point.

Each movement reached a target at a rate of 0.6 s/movement. W_{Ci} (i =1, 2, 3, 4) were zero matrices, and W_S was set to be the normalized arm matrix as in the initial conditions. W_{Ci} and W_S are updated by the adaptation rules in (19) and (22) in every trial. The trials are repeated until $|\varepsilon_{k+1}-\varepsilon_k|<10^{-6}$, where $\varepsilon = \int_{t_o}^{t_f}\sqrt{(x_d-x)^2+(y_d-y)^2}\,dt$.

Simulation results showed the effectiveness of the model to learn movements (Fig. 4(a)). In the Cartesian coordinate system, the trajectories were almost straight and included small hook-like stop motions at the ends. The profiles resembled natural human movements.

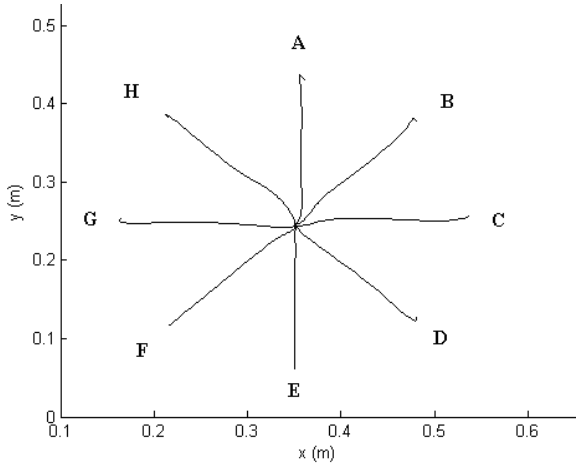

(a) Hand end movements.

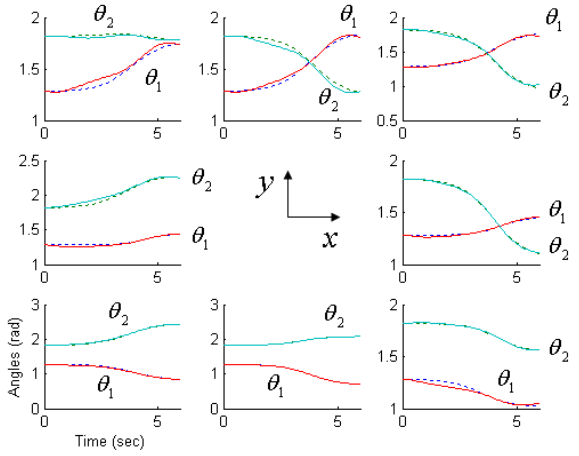

(b) Joint angle trajectories (dotted: desired; solid: actual).

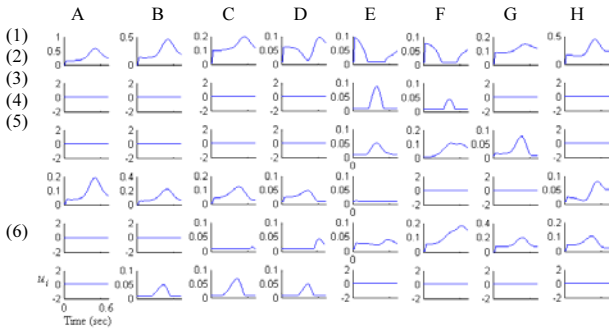

(c) Muscular activations.

Fig. 4. Simulated point-to-point reaching movements.

The convergence condition was achieved after 100 to 150 trials depending on directions; however, the motions were close to the final trajectories within 60 trials. The converged movements are described with respect to the joints in Fig. 4(b). The descending signal from the supraspinal and spinal system provided simulated muscular activations from (15), (18). Depending on the movement directions, different groups of muscles were activated. In Fig. 4(c), as movement directions changed from A to H, the activation profiles of each muscle changed gradually. The activation patterns were intuitively acceptable.

3.2. Curved movements: figure eight-like movements

Using the proposed model, figure eight-like drawings in two cases are tested. The desired hand end trajectories of the figure eight expressed in the Cartesian are:

$$1)\ x_d(t)=0.15\sin(\frac{\pi}{4}t)+0.35,\ y_d(t)=0.15\sin(\frac{\pi}{2}t)+0.25$$

$$2)\ x_d(t)=0.15\sin(\frac{\pi}{2}t)+0.35,\ y_d(t)=0.15\sin(\frac{\pi}{4}t)+0.25.$$

In both cases, all $W_{C,i}$ are zero matrices, and W_S is set to be normalized arm matrix as initial conditions. The trials are repeated until $|\varepsilon_{k+1}-\varepsilon_k|<0.00001$, where $\varepsilon = \int_{t_o}^{t_f}\sqrt{(x_d-x)^2+(y_d-y)^2}\,dt$. Figs. 5 and 6 demonstrate the simulated arm movements and muscular activations after adaptation. The movements follow their desired ones reasonably. In Figs. 5 and 6, an arrow indicates the starting direction, and the movement draws a figure eight continuously.

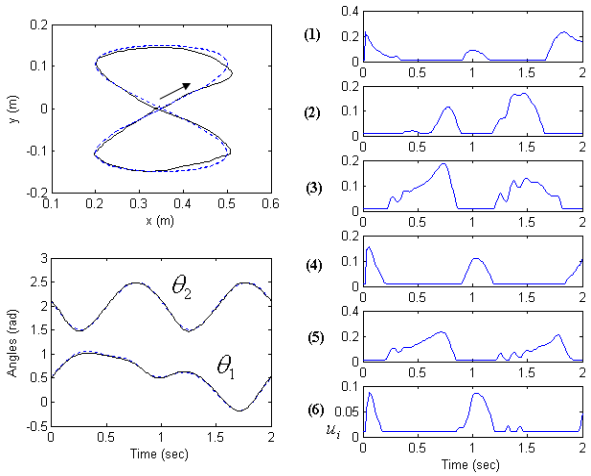

Fig. 5. Simulated arm movement with desired trajectory (1). (Left, top): hand end movement, (left, bottom): desired and simulated joint trajectories, (right): simulated muscular activation profiles. The dotted and solid lines represent desiredand simulated, respectively. Numbers indicate the corresponding muscles in Fig. 1.

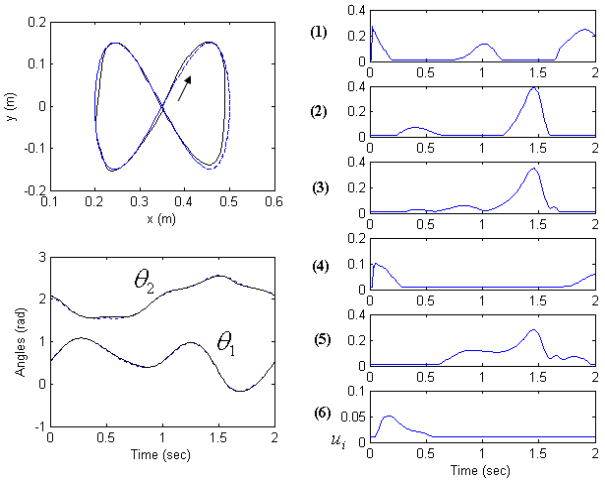

Fig. 6. Simulated arm movement with desired trajectory (2). (left, top): hand end movement, (left, bottom): desired and simulated joint trajectories, (right): simulated muscular activation profiles, dotted: desired, solid: simulated. Numbers indicate the corresponding muscles in Fig. 1.

4. DISCUSSION

In this paper, computational studies propose the following points. The criticism about the interpretation of cerebellar function as a feedforward inverse model was due to the computational complexity of the inverse model. In general, an inverse dynamics model requires information on physical parameters such as mass or length. However, this study demonstrates that such complicated computations based on inverse dynamics may not be necessary. A simple combination of kinematic states, probably allowing a little nonlinearity such as quadratic terms, is a sufficient approximation of the inverse model. Furthermore, the learning gains do not need to be related to physical parameters such as inertia or length. Although the inverse model information of the cerebellum may be quite rudimentary in comparison with general inverse model techniques in engineering, the spinal cord processing and muscle-tendon dynamics may be able to manipulate the descending commands to perform complicated tasks. An interpretation is that the inverse model computation is not only a unique role of the cerebellum, but the integrated mechanism of the overall neuromusculoskeletal system that carries out the computation. In the process, explicit information such as physical parameters seems unnecessary.

Generally, modeling studies of voluntary arm movements have been limited to point-to-point movements. This study demonstrates that slightly more complex (curved) arm movements such as figure eight-like movements at reasonably fast speeds can still be generated with either gain scheduling or highly precise inverse computation. Computational studies demonstrate that the FEL-type neural control system can generate the appropriate muscular activation to control the musculoskeletal system of arm movement. The proposed neuromusculoskeletal model can learn and generate realistic movements in spite of neural delays and neuromuscular dynamics.

This study assumes the idea that, to control redundant muscular actuators, synergy network processing may exist in the spinal cord. Many experimental studies have demonstrated such a possibility [7,11,12]. The spinal synergy network is considered an active motor system that adapts the distribution of descending signals to the muscles. The adaptive ability may be described by a type of Hebbian (Oja's) rule, i.e., unsupervised motor control. Appropriate connectivity and the degrees of intensity of the network are adaptively decided by long-term potentiation and depression through repetitive training sections. For a long training period, selection of an appropriate synergy network for a specific movement task would be required. Switching control is a potential scheme to explain the selection mechanism. In the cerebral cortex, motor control may perform switching to choose an appropriate set of synergy (W_S) or even further an appropriate microcomplex zone in the cerebellum (W_{Ci}). Such a modular scheme is theoretically studied in [6,46], and a possible switching neural mechanism in the cerebellar cortex is proposed in [47].

Further investigation will be required to improve the present model with a detailed modular motor control scheme. At least, this study here proposes a simple model of the hierarchical adaptation process performed in the spinal and supraspinal systems and demonstrates that the model can result in online successful learning of arm control. The adaptation at the supraspinal level is representatively modeled by FEL, and the adaptation at the spinal level is described by unsupervised learning. Both adaptations should be appropriately performed to achieve arm movement tasks successfully. In fact, spinalized cat experiments [21,22] demonstrate not only a unique motor system but also the interactive combination of spinal and supraspinal systems, which contribute to fully understanding the motor adaptation process in locomotion. Although this study tested voluntary arm movements, the model structure is consistent with the proposal from animal experiments. This neural structure may give insights on a simple motor control scheme of a redundant dynamics system and provide flexibility to control various movement tasks.

In this study, the unsupervised motor learning center was located, for simplicity, in the spinal system based on experimental observations of synergy. However, the location may be anywhere in the corticospinal neural pathway. The C3/C4 network [2,48] and spinal network in particular are possible locations (as expressed by a dotted box in Fig. 7). Moreover, synergy is just one out of many terms, e.g., primitives, modules, and unit bursters, to refer to "unit of motor output" as consisting of the coupled activation of a group of muscles [7]. An emphasis is on its role of transforming descending signals in controlling redundant muscles. Further investigation is required to confirm its location. It is also natural to think of the similar concept in the ascending pathway. In a general case, only useful information would be selected out of the massive sensory information

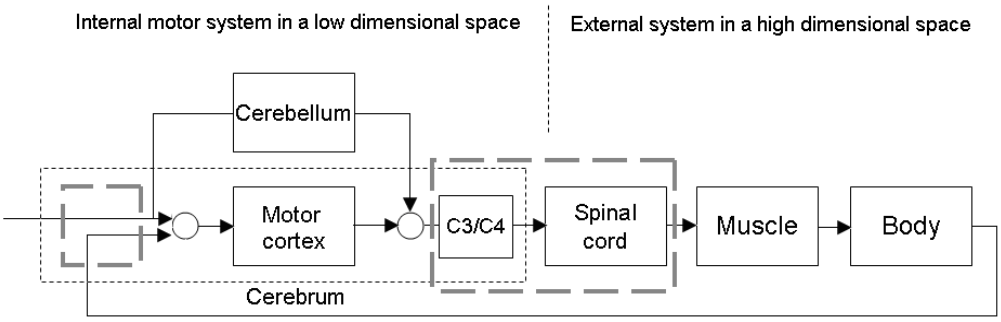

Fig. 7. Hypothetical sensorimotor control strategy with transformations in both ascending and descending neural pathways.

and sophisticated signal processing. Additionally, decoupled groups of signals may be sent to different sensorimotor regions to control different limbs simultaneously. Cortical neuronal columns in the cerebral cortical layers are characterized by their specific response tuning. During the arm movements of a monkey, directional tuning of neuronal discharges in the parietal and motor cortices are observed [49,50]. In the visual cortex, the response tuning depends on the orientation and color of the visual stimuli [51]. Furthermore, directional tunings of discharges in the cerebellar cortex, motor cortex, and parietal cortex are strikingly similar during arm reaching tasks [49,50,52]. In addition, it is also reported that directional tunings of Purkinje cells, interpositus neurons, dentate units, and unidentified cerebellar cortical cells are identical [53]. The experimental observations suggest the transformation of sensed or desired information in the cortex. The transformation may contrive the internal motor system in a lower dimensional space [49]. The transformation would be functionally opposite to the synergy network because it reduces dimensionality and enables adaptation for a specific task. Hebbian (Oja's) rules have also been used to model sensorimotor learning in the cortex [28,34]. Hypothetically, two transformations in ascending and descending neural pathways (Fig. 7) may be comparable with the encoder and decoder, respectively, to facilitate the control problem from a viewpoint of the motor system in a brain.

REFERENCES

[1] S. G. Massaquoi and H. Topka, "Models of cerebellar function," In Pandolfo, M & Manto, M. (ed.) *The Cerebellum and its Disorders*, pp. 69-94, Cambridge, U.K., Cambridge University Press, 2002.

[2] N. Schweighofer, M. A. Arbib, and M. Kawato, "Role of the cerebellum in reaching movements in humans, I. distributed inverse dynamics model," *European Journal of Neuroscience*, vol. 10, pp. 86-94, 1998.

[3] N. Schweighofer, M. A. Arbib, and M. Kawato, "Role of the cerebellum in reaching movements in humans, II. a neural model of the intermediate cerebellum," *European Journal of Neuroscience*, vol. 10, pp. 95-105, 1998.

[4] M. Kawato and H. Gomi, "A computational model of four regions of the cerebellum based on feedback-error learning," *Biological Cybernetics*, vol. 68, pp. 95-103, 1992.

[5] H. Gomi and M. Kawato, "Adaptive feedback control models of the vestibulocerebellum and spinocerebellum," *Biological Cybernetics*, vol. 68, pp. 105-114, 1992.

[6] M. Kawato, "Internal models for motor control and trajectory planning," *Current Opinion in Neurobiology*, vol. 9, pp. 718-727, 1999.

[7] E. Bizzi, M. C. Tresch, P. Saltiel, and A. d'Avella, "New perspectives on spinal motor systems," *Nature Neuroscience*, vol. 1, pp. 101-108, 2000.

[8] R. Poppele and G. Bosco, "Sophisticated spinal contributions to motor control," *Trends in Neuroscience*, vol. 25, no. 5, pp. 269-276, 2003.

[9] J. H. Martin, "The corticospinal system: from development to motor control," *The Neuroscientist*, vol. 11, no. 2, pp. 161-173, 2005.

[10] M. C. Tresch and O. Kiehn, "Coding of locomotor phase in populations of neurons in rostral and caudal segments of the neonatal rat lumbar spinal cord," *Journal of Neurophysiology*, vol. 82, pp. 3563-3574, 1999.

[11] P. Saltiel, K. Wyler-Duda, A. d'Avella, M. C. Tresch, and E. Bizzi, "Muscle synergies encoded within the spinal cord: evidence from focal intraspinal NMDA iontophoresis in the frog," *Journal of Neurophysiology*, vol. 85, pp. 605-619, 2001.

[12] A. d'Avella, P. Saltiel, and E. Bizzi, "Combinations of muscle synergies in the construction of a natural motor behavior," *Nature Neuroscience*, vol. 6, no. 3, pp. 300-308, 2003.

[13] V. C. K. Cheung, A. d'Avella, M. C. Treschm, and E. Bizzi, "Central and sensory contributions to the activation and organization of muscle synergies during natural motor behaviors," *Journal of Neuroscience*, vol. 25, no. 27, pp. 6419-6434, 2005.

[14] Y. P. Ivanenko, R. Grasso, M. Zago, M. Molinari, G. Scivoletto, V. Castellano, V. Macellari, and F. Lacquaniti, "Temporal components of the motor patterns expressed by the human spinal cord reflect foot kinematics," *Journal of Neurophysiology*, vol. 90, pp. 3555-3565, 2003.

[15] S. Jo and S. G. Massaquoi, "A model of cerebroce-

rebello-spinomuscular interaction in the sagittal control of human walking," *Biological Cybernetics*, vol. 96, no. 3, pp. 279-307, 2007.
[16] S. Jo, "A neurobiological model of the recovery strategies from perturbed walking," *Biosystems*, vol. 90, no. 3, pp. 750-768, 2007.
[17] S. Jo, "Hypothetical neural control of human bipedal walking with voluntary modulation," *Medical and Biological Engineering and Computing*, vol. 46, no. 2, pp. 179-193, 2008.
[18] J. Cheung, R. B. Stein, K. Jovanovic, K. Yoshida, D. J. Bennett, and Y. Han, "Identification, localization, and modulation of neural networks for walking in the mudpuppy (*Necturus maculates*) spinal cord," *Journal of Neuroscience*, vol. 18, pp. 4295-4304, 1998.
[19] K. G. Pearson and S. Rossignol, "Fictive motor patterns in chronic spinal cats," *Journal of Neurophysiology*, vol. 66, pp. 1874-1887, 1991.
[20] P. S. Stein, M. L. McCullough, and S. N. Currie, "Spinal motor patterns in the turtle," *Annals of the New York Academy of Sciences*, vol. 16, pp. 142-154, 1998.
[21] P. J. Whelan and K. G. Pearson, "Plasticity in reflex pathways controlling stepping in the cat," *Journal of Neurophysiology*, vol. 78, pp. 1643-1650, 1997.
[22] L. Carrier, E. Brustein, and S. Rossignol, "Locomotion of the hindlimbs after neurectomy of ankle flexors in intact and spinal cats: model for the study of locomotor plasticity," *Journal of Neurophysiology*, vol. 77, pp. 1979-1993, 1997.
[23] R. Grasso, Y. P. Ivanenko, M. Zago, M. Molinari, G. Scivoletto, V. Castellano, V. Macellari, and F. Lacquaniti, "Distributed plasticity of locomotor pattern generators in spinal cord injured patients," *Brain*, vol. 127, pp. 1019-1034, 2004.
[24] J. M. Winters, "Hill-based muscle model: a system engineering perspective," In J.M. Winters & SL-Y. Woo (Eds), *Multiple Muscle Systems, biomechanics and movement organization*, pp. 69-93, Springer Verlag, New York.Yamaguchi, G. T., Sawa, A. G. U., Moran, D. W., Fessler, 1990.
[25] F. E. Zajac, "Muscle and tendon: properties, models, scaling, and application to biomechanics and motor control," In J. Bourne (ed), *CRC Critical Reviews in Biomedical Engineering*, vol. 17, pp. 359-411, CRC Press, Boca Raton, 1989.
[26] H. Imamizu, S. Myauchi, T. Tamada, Y. Sasaki, R. Takino, B. Puetz, T. Yoshioka, and M. Kawato, "Human cerebellar activity reflecting an acquired internal model of a novel tool," *Nature*, vol. 403, pp. 192-195, 2000.
[27] J. Nakanishi and S. Schaal, "Feedback error learning and nonlinear adaptive control," *Neural Networks*, vol. 17, no. 10, pp. 1453-1465, 2004.
[28] K. Doya, "What are the computations of the cerebellum, the basal ganglia, and the cerebral cortex?," *Neural Networks*, vol. 12, no. 7, pp. 961-974, 1999.
[29] H. Gomi and M. Kawato, "Learning control for a closed loop system," *Proc. of the 29th Conference on Decision & Control*, Honolulu, Hawaii, USA, pp. 3289-3294, 1990.
[30] M. Ito, "Neural design of the cerebellar motor control system," *Brain Research*, vol. 40, pp. 81-84, 1972.
[31] J. Spoelstra, N. Schweighofer, and M. A. Arbib, "Cerebellar learning of accurate predictive control for fast-reaching movements," *Biological Cybernetics*, vol. 82, pp. 321-333, 2000.
[32] J. L. Contreras-Vidal, S. Grossberg, and D. Bullock, "Neural model of cerebellar learning for arm movement control: cortico-spino-cerebellar dynamics," *Learning Memory*, vol. 3, pp. 475-502, 1997.
[33] R. Holdefer and L. Miller, "Primary motor cortical neurons encode functional muscle synergies," Experimental Brain Research, vol. 146, no. 2, pp. 233-243, Sep. 2002.
[34] L. F. Abbott and S. B. Nelson, "Synaptic plasticity: taming the beast," *Nature Neuroscience*, vol. 3, pp. 1178-1183, 2000.
[35] Y. Lo and M. Poo, "Activity-dependent synaptic competition *in vitro*: heterosynaptic suppression of developing synapses," *Science*, vol. 254, pp. 1019-1022, 1991.
[36] P. K. Stanton and T. J. Sejnowski, "Associative long-term depression in the hippocampus induced by Hebbian covariance," *Nature*, vol. 229, pp. 215-218, 1989.
[37] R. J. O'Brien, S. Kamboj, M. D. Ehlers, K. R. Rosen, G. D. Fischbach, and R. L. Huganir, "Activity-dependent modulation of synaptic AMPA receptor accumulation," *Neuron*, vol. 21, pp. 1067-1078, 1998.
[38] D. T. Davy and M. L. Audu, "A dynamic optimization technique for predicting muscle forces in the swing phase of gait," *Journal of Biomechanics*, vol. 20, pp. 187-201, 1987.
[39] N. Ogihara and N. Yamazaki, "Generation of human reaching movement using a recurrent neural network model," *Conference Proceedings of System, Man, and Cybernetics*, pp. 692-697, 1999.
[40] M. A. Lemay and P. E. Crago, "A dynamic model for simulating movements of the elbow, forearm, and wrist," *Journal of Biomechanics*, vol. 29, pp. 1319-1330, 1996.
[41] S. Delp, *Surgery Simulation: A Computer Graphics System to Analyze and Design Musculoskeletal Reconstructions of the Lower Limb*, Ph.D. Thesis, Mechanical Engineering, Stanford University, Palto Alto, CA, USA, 1999.
[42] A. J. van Soest and M. F. Bobbert, "The contribution of muscle properties in the control of explosive movements," *Biological Cybernetics*, vol. 69, pp. 195-204, 1993.
[43] H. Geyer, A. Seyfarth, and R. Blickhan, "Positive force feedback in bouncing gaits?," *Proc. of the Royal Society B: Biological Sciences*, vol. 270, pp. 2173-2183, 2003.
[44] M. Günther and H. Ruder, "Synthesis of two-dimensional human walking: a test of the λ-model,"

Biological Cybernetics, vol. 89, pp. 89-106, 2003.
[45] F. C. Anderson and M. G. Pandy, "Static and dynamic optimization solutions for gait are practically equivalent," *Journal of Biomechanics*, vol. 34, pp. 153-161, 2001.
[46] M. Haruno, D. M. Wolpert, and M. Kawato, "MOSAIC model for sensorimotor learning and control," *Neural Computation*, vol. 13, pp. 2201-2220, 2001.
[47] S. Jo and S. G. Massaquoi, "A model of cerebellum-stabilized and scheduled hybrid long-loop control of upright balance," *Biological Cybernetics*, vol. 91, no. 3, pp. 188-202.
[48] B. Alstermark, A. Lundberg, U. Norrsell, and E. Sybirska, "Integration in descending motor pathways controlling the forelimb in the cat. IX. Differential behavioral defects after spinal cord lesions interrupting defined pathways from higher centres to motoneurones," *Experimental Brain Research*, vol. 42, pp. 299-318, 1981.
[49] J. F. Kalaska, R. Caminiti, and A. P. Georgopoulos, "Cortical mechanisms related to the direction of two-dimensional arm movements: relations in parietal area 5 and comparison with motor cortex," *Experimental Brain Research*, vol. 51, pp. 247-260, 1983.
[50] A. Georgopouls, J. F. Kalaska, R. Caminiti, and J. T. Massey, "On the relations between the direction of two-dimensional arm movements and cell discharge in primate motor cortex," *Journal of Neuroscience*, vol. 2, pp. 1527-1537, 1983.
[51] H. V. B. Hirsch and D. N. Spinelli, "Visual experience modifies distribution of horizontally and vertically oriented receptive fields in cat," *Science*, vol. 168, pp. 869-871, 1970.
[52] R. C. Frysinger, D. Bourbonnais, J. F. Kalaska, and A. M. Smith, "Cerebellar cortical activity during antagonist cocontraction and reciprocal inhibition of forearm muscles," *J. Neurophysiol.*, vol. 51, pp. 32-49, 1984.
[53] P. A. Fortier, J. F. Kalaska, and A. M. Smith, "Cerebellar neuronal activity related to whole-arm reaching movements in the monkey," *Journal of Neurophysiology*, vol. 62, no. 1, pp. 198-211, 1989.

Sungho Jo received his B.S. degree in the School of Mechanical & Aerospace Engineering of Seoul National University, Seoul, Korea, in 1999. He completed an M.S. degree in Mechanical Engineering and Ph.D. degree in Electrical Engineering and Computer Science from Massachusetts Institute of Technology, Cambridge, MA, in 2001 and 2006, respectively. From 2006 to 2007, he was a Postdoctoral Researcher at the MIT Media Lab, Cambridge, MA. Since 2007, he has been an Assistant Professor in the Department of Computer Science at KAIST, Korea. His research interests include human-robot interaction, intelligent robotics, and biomedical robotics.